CHEMISTRY

Noncontact catalysis: Initiation of selective ethylbenzene oxidation by Au cluster-facilitated cyclooctene epoxidation

Anyang Peng[1], Mayfair C. Kung[1]*, Robert R. O. Brydon[1], Matthew O. Ross[2], Linping Qian[3], Linda J. Broadbelt[1], Harold H. Kung[1]*

Traditionally, a catalyst functions by direct interaction with reactants. In a new noncontact catalytic system (NCCS), an intermediate produced by one catalytic reaction serves as an intermediary to enable an independent reaction to proceed. An example is the selective oxidation of ethylbenzene, which could not occur in the presence of either solubilized Au nanoclusters or cyclooctene, but proceeded readily when both were present simultaneously. The Au-initiated selective epoxidation of cyclooctene generated cyclooctenyl peroxy and oxy radicals that served as intermediaries to initiate the ethylbenzene oxidation. This combined system effectively extended the catalytic effect of Au. The reaction mechanism was supported by reaction kinetics and spin trap experiments. NCCS enables parallel reactions to proceed without the constraints of stoichiometric relationships, offering new degrees of freedom in industrial hydrocarbon co-oxidation processes.

INTRODUCTION

Traditionally, a catalyst interacts directly with the reactants (reaction A) to effect bond rearrangements prescribed by the reaction. For example, in the cobalt-catalyzed oxidation of alkylaromatics (*1*) or the Au-catalyzed epoxidation of cyclooctene (*2*), the catalyst facilitates abstraction of a hydrogen atom from the hydrocarbon to initiate the reaction. In a free radical chain reaction, a catalyst participates in catalytic homolytic cleavage of a weak bond in the initiators that are either added intentionally or present as adventitious impurities in the reaction mixture (*1*, *3*, *4*). Some steps in a catalytic tandem reaction may not require direct substrate-catalyst contact when the transformation of the substrate is enabled by product produced catalytically in preceding steps (*5*–*8*). However, these reactions are constrained by the stoichiometric relationships between the steps. For example, in the Mukaiyama (ep)oxidation of an alkene, a catalyst converts a sacrificial reductant in reaction A, such as isobutyraldehyde, with the concomitant stoichiometric formation of an epoxide (reaction B) (*9*, *10*). Although possible in principle, we are not aware of an example in which the function of a catalyst is to produce an intermediate S in reaction A, where S serves as an intermediary to either initiate or catalyze another reaction B instead of participating as a stoichiometric reagent, while the catalyst is not effective for reaction B (Fig. 1). In such a scheme, the influence of the catalyst is extended beyond catalyzing reaction A to also effecting reaction B but without direct contact with its reactants. We term such a scheme a noncontact catalytic system (NCCS). In NCCS, the extents of reaction of reactions A and B are not bound by any stoichiometric relationship between them. This is in contrast to tandem reactions. In industry, such a stoichiometric relationship often imposes economic constraints on a chemical production process. A well-known example is the stoichiometric production of phenol and acetone by oxidation of benzene via a cumene hydroperoxide intermediate in the cumene process (*11*).

RESULTS AND DISCUSSION

We found such an NCCS when exploring the catalytic properties of solubilized Au_n clusters (where n was mostly six to eight atoms) for partial oxidation of ethylbenzene (EB). We have demonstrated that these solubilized Au_n catalyzed the initiation of selective epoxidation of cyclooctene (cC_8=) with O_2 with ~80% selectivity (*2*). These clusters were formed in situ during Au/SiO_2-catalyzed cC_8= epoxidation, and they maintained their ability to generate the radical initiator cyclooctene hydroperoxy radical (cC_8=OO·) throughout the reaction. The solubilized Au_n clusters could be collected in the reaction mixture after removal of Au/SiO_2, and their average size was determined using aberration-corrected electron microscopy and fluorescence spectroscopy (*2*). In addition to Au_n clusters, these mixtures also contained cyclooctene hydroperoxide (cC_8=OOH) and oxidation products cyclooctene epoxide, cyclooctenol, and cyclooctenone. cC_8=OOH was the stable hydrogenated form of cC_8=OO· and present at concentrations of 0.2 to 0.5 M after 40 to 100% cC_8= conversion. This mixture is referred to as Au + cC_8=OOH-x,

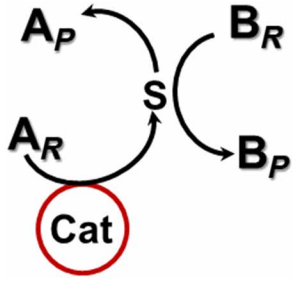

Fig. 1. A noncontact catalytic system. A catalyst (Cat) catalyzes reaction A (A_R ➔ S ➔A_P) in which the intermediate S is effective in either initiating or catalyzing reaction B (B_R ➔ B_P), although reaction B is not catalyzed by the catalyst.

[1]Department of Chemical and Biological Engineering, Northwestern University, Evanston, IL 60208, USA. [2]Department of Chemistry, Northwestern University, Evanston, IL 60208, USA. [3]Department of Chemistry, Laboratory of Advanced Materials and Collaborative Innovation Center of Chemistry for Energy Materials, Fudan University, 2005 Songhu Road, Shanghai 200438, China.
*Corresponding author. Email: hkung@northwestern.edu (H.H.K.); m-kung@northwestern.edu (M.C.K.)

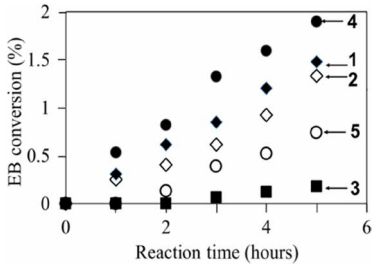

Fig. 2. Conversion of EB as a function of time in different cyclooctene (cC_8=) mixtures. (i) 7 ml of EB + 3 ml of Au + cC_8=OOH-50; (ii) 7 ml of EB + 3 ml of Au + cC_8=OOH-50 + 1.2 mmol PPh_3; (iii) 7 ml of EB + 3 ml of Au + cC_8=OOH-99 + 0.6 mmol PPh_3; (iv) 7 ml of EB + 3 ml of cC_8=OOH-50; (v) 7 ml of EB + 3 ml of cC_8=OOH-50 + 1.5 mmol PPh_3. Quantity of PPh_3 added was set to equal the quantity of titrated hydroperoxide (reaction temperature, 100°C).

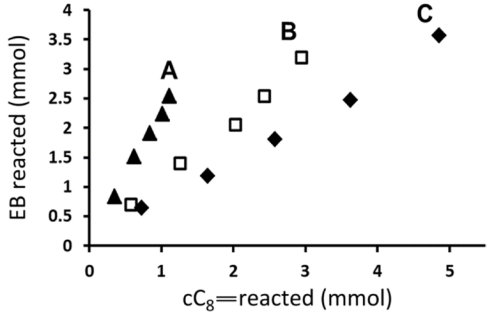

Fig. 3. Quantity of EB and cyclooctene reacted in experiments with fixed initial concentrations of EB (5 M), Au_n, and cC_8=OOH. Initial cC_8= concentrations were 0.34 M (A), 1.05 M (B), and 1.75 M (C). Decane was used to make up the differences in volume of cC_8= used. Other conditions: 32 mg of Co/ZSM5, 100°C.

where x is the percent cC_8= conversion. Although at a much slower rate and with a long (>5 hours) induction period, cC_8= epoxidation could also occur by auto-oxidation without Au_n clusters. Mixtures obtained by auto-oxidation without Au are called cC_8=OOH-x. In the NCCS, the solubilized Au_n would be the catalyst, the epoxidation of cC_8= would be reaction A, and cC_8=OO· would be S.

The auto-oxidation of EB does not occur readily. At 145°C, only 9% reaction occurred for neat EB under 2.76 MPa O_2 (*12*). Under our much milder conditions of 100°C and bubbling O_2 at 0.1 MPa, there was no detectable reaction of neat EB for at least 20 hours. Addition of a free radical initiator was required for this reaction to proceed. Initiation with 2,2′-azobisisobutyronitrile (AIBN), a highly reactive thermal radical initiator, resulted in auto-oxidation of EB with an average chain length of ~3 (fig. S2A). A shorter (~1) chain was observed using the less active *tert*-butyl hydroperoxide (fig. S2B), and there was very little detectable reaction using the least active cumene hydroperoxide. Thus, auto-oxidation of EB had little influence on the reaction results reported below.

A steady aerobic oxidation of EB to EB hydroperoxide, acetophenone, and phenylethanol was achieved by adding Au + cC_8=OOH-50 containing a mixture of Au_n, cC_8=OOH, and unreacted cC_8= (Fig. 2, curve 1). As demonstrated by the following experiments, these three components played principal roles in EB oxidation, and they corresponded to catalyst, S, and A_R in the NCCS system depicted in Fig. 1.

Under our conditions, no observable aerobic EB oxidation occurred in a mixture of cC_8= and EB (i.e., without Cat or S). Triphenylphosphine (PPh_3) is very effective in removing hydroperoxides. A Au + cC_8=OOH-99 solution, depleted of cC_8=OOH by PPh_3 addition, containing Au_n and very little unreacted cC_8=, failed to initiate the EB reaction even after 2 hours (Fig. 2, curve 3), indicating that Au_n alone was ineffective. This result also indicated that other products of cC_8= oxidation, such as cyclooctene epoxide, cyclooctene alcohol, or ketone, were not able to initiate EB oxidation. In contrast to the above experiment, removal of cC_8=OOH with PPh_3 from Au + cC_8=OOH-50, leaving behind Au_n and unreacted cC_8=, did not deter EB conversion (compare curves 1 and 2, Fig. 2).

These three sets of data suggested synergism between Au_n and unreacted cC_8= in the initiation of EB oxidation. We hypothesized that Au_n catalyzed the oxidation of cC_8= to form cC_8=OOH, which was the initiator of EB reaction. This could be tested by comparing the efficiency of initiating EB oxidation with a mixture of cC_8=OOH and cC_8= but without Au_n before and after removal of cC_8=OOH with PPh_3. To best mimic the conditions of the earlier sets of experiments, we used the solution cC_8=OOH-50 for the mixture of cC_8=OOH and cC_8= so that any possible effect of cC_8= epoxidation products would be reproduced. The results showed that in the presence of cC_8=OOH-50, EB reacted efficiently (Fig. 2, curve 4). However, if cC_8=OOH was removed by PPh_3, there was no reaction for the first hour and suppressed activity subsequently (curve 5). These data further supported the model that the catalytic role of Au_n was to continuously generate cC_8=OOH via cC_8= oxidation, and cC_8=OOH initiated the EB reaction. The catalytic role of Au_n was further confirmed by observing that the initial rates of EB oxidation in the absence of cC_8=OOH increased with increasing Au_n concentration (fig. S3).

The unique role of Au_n in this NCCS was demonstrated by examining Co as an alternate catalyst, which was chosen because cobalt acetate and cobalt cycloalkanecarboxylate (*13*) are industrial catalysts for conversion of EB to acetophenone with molecular O_2, operating under harsh conditions and requiring the presence of acid and bromide ions. Co complexes are also used for selective aerobic EB oxidation in the presence of an organocatalyst *N*-hydroxyphthalimide (NHPI) or a sacrificial reductant (*14*, *15*). However, under our reaction conditions, the presence of Co/ZSM-5 did not result in any detectable oxidation of EB, cC_8=, or their mixture for at least 6 hours. That is, Co alone could not initiate either oxidation reaction. However, in the presence of both Au_n and cC_8=, it facilitated the oxidation reactions. Depending on the condition, cC_8= or EB reacted three to five times faster when Co/ZSM-5 was present, and the enhancement increased with the amount of Co/ZSM-5 (table S2, experiments 6 to 8). The EB oxidation product distribution also changed somewhat in the presence of Co/ZSM-5. Increasing the amount of Co/ZSM-5 increased the acetophenone yields and, to a lesser extent, phenylethanol yields at the expense of EB hydroperoxide (table S3, experiments 6 to 8), consistent with the fact that Co catalyzed decomposition of EB hydroperoxide to acetophenone and phenylethanol and the oxidation of the latter to acetophenone. For the sake of expediency, we included Co/ZSM-5 in our reaction mixture to shorten the reaction time.

A distinguishing factor between NCCS and tandem reaction systems is that in the former, there is no stoichiometric relationship between reactions A and B (Fig. 1). To validate that our reactions occurred via NCCS, we tested the effect of changing the ratio of cC_8= to EB by monitoring their individual reaction rates. Figure 3

Table 1. Initial rates and product distributions during simultaneous reactions of EB and cyclooctene.

Initial amounts (M)*		Initial rates (M/hour)†		Initial selectivities (%)†,‡			
cC_8=	EB	cC_8=	EB	cC_8= oxide,§	EBOOH	Acetophenone	1-Phenylethanol
0.35	5.2	0.016 ± 0.002	0.036 ± 0.003	87	57	14	29
1.1	5.2	0.027 ± 0.003	0.033 ± 0.003	86	54	16	30
1.8	5.2	0.037 ± 0.004	0.027 ± 0.003	87	58	17	25

*Initial quantities in the reaction mixture, total volume (11 ml) consisted of 1.5 ml of cC_8=OOH-50, the indicated amounts of cC_8= and EB, and balance decane, 32 mg of Co/ZSM-5, 100°C. †Determined from data with <15% conversion. ‡Selectivities of the products that formed separately from cC_8= (cC_8= oxide) and EB (EBOOH, acetophenone, and 1-phenylethanol). §The remaining cC_8 products were cyclooctenone and cyclooctenol.

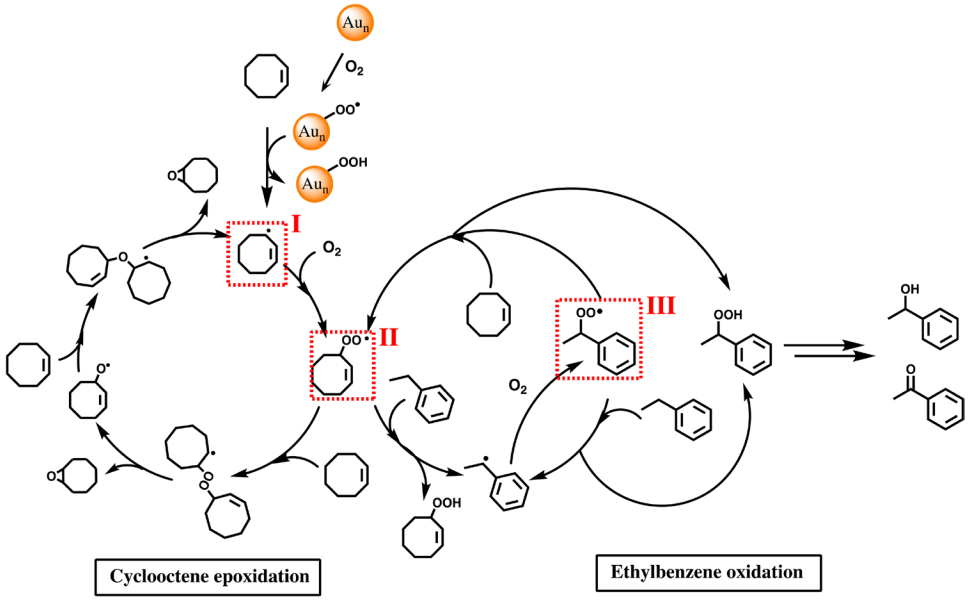

Fig. 4. Mechanistic scheme for the NCCS for the oxidation of EB facilitated by Au$_n$-catalyzed epoxidation of cyclooctene. Cyclooctene peroxy radical (**II**) is the principal intermediary that initiates the EB oxidation. **II** can be regenerated by reaction of EB peroxy radical (**III**) with cC_8=. On the top left, Au$_n$ clusters initiate the cC_8= epoxidation cycle (cycle on the left). The cycle on the right shows the steps for EB oxidation. Only the principal steps important for NCCS are shown.

shows the results of changing the initial cC_8= concentration while keeping the initial EB concentration and other reaction conditions constant. The data show that there was no fixed stoichiometric relationship between the quantities of the two reactants reacted, confirming that the reaction pattern differed from the traditional tandem reaction scheme. An analogous set of experiments in which the initial EB concentrations were varied while fixing other concentrations arrived at the same conclusion. From these data, the initial reaction rates were calculated (Table 1 and table S2, experiments 4 and 5) and shown to vary differently for cC_8= and EB. There was no trade-off in reaction rates between the two reactions such that when one reaction proceeded faster, the other had to be slower proportionally. Both reaction rates could increase simultaneously, as shown by experiments 4 and 5 in table S2. A trade-off would be expected if EB and cC_8= competed for the same catalytic reaction site or intermediate. This conclusion is also consistent with the fact that the simultaneous reactions of EB and cC_8= had no or very small effect on their individual product distribution, as shown in Table 1 and table S3.

These data are consistent with the mechanistic scheme shown in Fig. 4, in which steps important for NCCS are emphasized and the principal players are highlighted (a more complete scheme is shown in fig. S8). In this mechanism, the Au$_n$ clusters initiate the cC_8= epoxidation cycle by generating cyclooctenyl radicals (**I**) and cyclooctene peroxy radicals (**II**). These two radicals then participate in the cC_8= epoxidation cycle, as was established previously (*2*, *16*). When EB is present, **II** becomes an intermediary molecule and shuttles between the cC_8= epoxidation cycle and the EB oxidation cycle. In the EB cycle, **II** reacts with EB to form a phenylethyl radical, which immediately forms a phenylethyl peroxy radical (**III**) by reaction with O_2, as carbon-centered radical reactions with O_2 are known to be extremely facile (*1*). Subsequent hydrogen abstraction by **III** forms phenylethyl hydroperoxide and eventually acetophenone and phenylethanol. **III** can also react rapidly with cC_8=, which becomes the pathway to replenish **II** that is consumed by the EB oxidation cycle. Thus, the EB oxidation reaction is not accompanied by a stoichiometric suppression of the cC_8= epoxidation reaction, and there is no "trade-off" in the reaction rates of EB and cC_8= as would be expected if they had

competed for the same reagent or catalytic active site. Because **II** participates in the initiation step in both EB and cC_8= oxidation cycles but not directly in the product formation steps, its bridging of the two reactions does not affect the product distributions.

To verify the formation of transient radical intermediates as proposed in Fig. 4, we added the spin trap 5,5-dimethyl-1-pyrroline *N*-oxide (DMPO) to the reaction mixture to form long-lived nitroxide radical spin adducts with the free radicals present for detection with X-band electron paramagnetic resonance (EPR) spectroscopy. As a control, no radicals were trapped by DMPO in a solution of acetone and decane without C8= or EB (fig. S4-3). When DMPO was added to a reaction mixture containing cC_8=OOH and cC_8= (fig. S4-1), the resultant EPR spectrum was well simulated as a sum of a major distinct paramagnetic species (*A* in the figure, ~86% of total simulation intensity) and two minor species (*B* and *C*, ~5 and ~9% of total simulation intensity, respectively), providing direct evidence of radical formation during the reaction. On the basis of comparison of the hyperfine coupling values to those of known DMPO adducts (table S1), species *C* was assigned to a DMPO/ROO$^\bullet$ adduct, plausibly the cyclooctene 3-peroxy radical (**II**) depicted as the intermediary between the two reactions (Fig. 4). Species *A* and *B* were assigned to two slightly different DMPO/RO$^\bullet$ adducts, where R referred to a hydrocarbon moiety. They could be one of the RO$^\bullet$ species described in Fig. 4 or alkoxy radicals produced from DMPO/ROO$^\bullet$ adduct decay [DMPO/ROO$^\bullet$ adducts are known to be unstable and decompose to the corresponding alkoxy radical adduct (*17*, *18*)] or a mixture of both. When EB was also included in the reaction mixture, the resultant EPR spectrum was well simulated with a majority species *A′*, which was very similar to species *A* (DMPO/RO$^\bullet$), and the two minority species *B* and *C* with similar minor contributions (fig. S4-2 and table S1). Because inclusion of EB was expected to drive the formation of phenylethyl peroxy radicals (**III**), species *A′* was likely a mixture of RO$^\bullet$ generated in the reaction as well as any phenylethyl peroxy adduct, which subsequently decayed to the phenylethyl oxy DMPO adduct.

Using EB-d_{10} as a reactant and monitoring deuterium labeling in cC_8= products could detect whether there was reaction of EB with cC_8= based carbon radicals. The results of such an experiment showed that there was no deuterium incorporation in cyclooctene epoxide (figs. S5 and S6). Phenylethanol retained all of the deuterium in the EB reactant, and some of the deuterons in the methyl group of acetophenone had exchanged, which could occur in the mass spectrometer. Thus, there was no evidence of reaction between EB-d_{10} and cyclooctenyl radical, which would introduce deuteron into cC_8= products.

The applicability of the NCCS strategy was extended to examine the Au + cC_8=OOH-100–assisted aerobic oxidation of 4-methylanisole. Because of the stronger primary C—H bonds in this molecule, the oxy-functionalization reaction was conducted at a higher temperature. The initial rates of conversion of 4-methylanisole to 4-anisaldehyde were compared for reactions initiated with Au_n and either with or without cC_8= addition (cC8=OOH was removed with PPh_3). Similar to EB oxidation, when the reaction mixture contained no cC8= and no cC_8=OOH, the initial oxidation rate was very slow (fig. S7). When cC_8= was added to the reaction mixture, the initial oxidation rate was noticeably enhanced. Thus, the Au_n clusters were able to generate cC8=OOH from the added cC_8= to initiate oxidation of 4-methylanisole as expected in NCCS.

In conclusion, we have demonstrated the concept of an NCCS. Using simultaneous oxidation of cyclooctene and EB as well as cyclooctene and 4-methylanisole, NCCS was shown to enable co-oxidation of hydrocarbons without the stoichiometric relationship constraints of the traditional co-oxidation processes. This offers a previously unavailable degree of freedom in industrial practice such that the process economics are no longer bound by the need for favorable markets for coproducts generated in stoichiometric amounts.

MATERIALS AND METHODS

Chemicals and materials

Sources and purities of chemicals used were as follows: $HAuCl_4 \cdot 3H_2O$ (≥99.9% trace metals basis, Sigma-Aldrich), fumed silica (CAB-O-SIL90, Cabot Corporation), ethylenediamine (≥99% ReagentPlus, Sigma-Aldrich), ethanol (200 grade, Decon Labs), cobalt(II) nitrate hexahydrate (≥98%, Sigma-Aldrich), Nano H-ZSM-5 (P-26, ACS Material), decane (≥99% ReagentPlus, Sigma-Aldrich), dodecane (≥99% ReagentPlus, Sigma-Aldrich), cis-cyclooctene (95%, Alfa Aesar), EB (99.8% anhydrous, Sigma-Aldrich), EB-d_{10} (99 atomic % D, Sigma-Aldrich), 4-methylanisole (99%, Sigma-Aldrich), acetophenone (99% ReagentPlus, Sigma-Aldrich), 1-phenylethanol (98%, Sigma-Aldrich), hydrogen peroxide (30% aqueous solution, Fisher Chemical), potassium hydroxide (reagent grade, 90%, Sigma-Aldrich), sodium sulfate (Food Chemicals Codex/United States Pharmacopeia–grade, Fisher Chemical), tetrahydrofuran (>99%, Sigma-Aldrich), *tert*-butyl hydroperoxide (~5.5 M in decane, Sigma-Aldrich), PPh_3 (>98.5%, Sigma-Aldrich), D-chloroform (99.8 atomic % D, Sigma-Aldrich), HCl (38% w/w, Fisher Chemical), HNO_3 (68 to 70% w/w, Fisher Chemical), EM Quant peroxide test strips, and syringe filter (polyvinylidene difluoride membrane, 0.25 mm/0.2 μm, Acrodisc).

Catalyst preparation and characterization

Au/SiO₂

The silica-supported gold nanoparticle catalyst was prepared with $Au(en)_2Cl_3$ precursor according to the method developed by Zhu *et al.* (*19*) and modified by Qian *et al.* (*2*). To be more specific, a Au(III) chloride trihydrate solution was prepared by dissolving 0.5 g of $HAuCl_4 \cdot 3H_2O$ in a mixture containing 10 ml of ethanol and 2 ml of water. After forming a homogeneous solution, 0.23 ml of ethylenediamine (en = ethylenediamine) was added to the solution dropwise to form Au(III) ethylenediamine chloride [$Au(en)_2Cl_3$] by ligand exchange. The as-formed $Au(en)_2Cl_3$ was collected by filtration and washed with 300 ml of ethanol. To deposit Au onto the silica support, a 4.2 mM $Au(en)_2Cl_3$ aqueous solution was prepared by dissolving 46.3 mg of $Au(en)_2Cl_3$ into 26 ml of distilled deionized (DDI) water. The as-formed solution was maintained at 40°C in an oil bath. Then, 1 g of fumed silica was added to the preheated solution while stirring. Once all the silica supports were immersed in the solution, the mixture was removed from the oil bath and cooled to room temperature. By adjusting the pH of the mixture to 9 with dropwise addition of 0.75 M en aqueous solution, a better adsorption of the cationic gold complexes to the negatively charged surface was achieved. After stirring for 2 hours at room temperature, the mixture was filtered and washed with 500 ml of DDI water. To remove unwanted residuals (Cl, en, other impurities), the filter cake was redispersed in 200 ml of DDI water at 40°C. Last, the as-formed Au/SiO_2 was collected by filtration and washed with another 500 ml of DDI water and dried in air overnight. Calcination of the silica-supported gold nanoparticles catalyst was carried out in a U-tube under O_2/O_3 flow (~300 ml/min) with a ramping rate of

0.12°C/min until 150°C. The catalyst was stored in the dark at 5°C. Gold loading, as quantified by inductively coupled plasma optical emission spectrometry, was 1.2 weight % (wt %), and the average gold particle size measured by scanning transmission electron microscopy (STEM) was around 2 nm.

Co/ZSM-5

Nano H-ZSM-5 was calcined in a U-tube under O_2/O_3 flow (~300 ml/min) with a ramping rate of 2°C/min until 200°C and held at 200°C for 1 hour to remove residual templates. Co/ZSM-5 was prepared by incipient wetness. For example, a 5 wt % loading Co/ZSM-5 was prepared by adding a 0.72 M cobalt (II) nitrate solution [250 mg of cobalt(II) nitrate hexahydrate in 1.2 ml of DDI water] to 1 g of nano H-ZSM-5 while carefully rotating the beaker. The slurry was dried under a lamp, and a uniform pink powder was formed. The as-formed powder was then loaded into a straight calcination tube and purged under argon flow (100 ml/min) for 1 hour to minimize humidity. The as-prepared catalyst was then calcined under oxygen flow (60 ml/min) with a ramping rate of 10°C/min to 450° (held at 250°C, 350°C, and 450°C for 1 hour each). The obtained Co/ZSM-5 has a cobalt loading of 5 wt %. Two other loadings, 3 and 7 wt %, were also prepared. All three catalysts were characterized by H_2 temperature-programmed reduction, x-ray diffraction, x-ray photoelectron spectroscopy, and ultraviolet-visible spectroscopy.

Au-containing filtrate

The Au-containing filtrate (Au + cC_8=OOH-*x*) was in situ generated from Au/SiO_2-catalyzed cC_8= epoxidation reaction according to the procedure developed by Qian *et al.* (*2*) Before reaction, cC_8= was purified to remove the manufacturer-added stabilizer. In general, 50 ml of 3 M potassium hydroxide (KOH) solution was added to 50 ml of cC_8= in a flask. After sufficient mixing and vigorous stirring, the organic layer was collected by separation. This procedure was repeated with another 50 ml of 3 M KOH and two other 50 ml of DDI water. The cC_8= was then dried with sodium sulfate overnight. To completely remove the stabilizer, the dried cC_8= was distilled in an oil bath at around 180°C, and the fraction that came out at 145°C was collected. Purified cC_8= (10 ml) and decane (1 ml) were mixed in a reactor containing 80 mg of the aforementioned Au/SiO_2 catalyst. The cC_8= epoxidation reaction was conducted under an oxygen flow (30 ml/min) at 100°C, and the conversion was monitored by GC. Once the desired conversion was reached, the reaction mixture was collected and the solid catalyst was removed by hot filtration using a syringe filter. The typical solubilized Au concentration that was determined by inductively coupled plasma mass spectrometry was about 80 ng/ml, and the Au cluster size was determined by fluorescence spectroscopy and aberration-corrected transmission electron microscopy ranging from Au atoms to ~0.7 nm. cC_8=OOH-*x* was prepared similarly without using the Au/SiO_2 catalyst. Both Au + cC_8=OOH-*x* and cC_8=OOH-*x* solutions contained cC_8= oxidation products, which included cyclooctene oxide, cyclooctene 3-hydroperoxide, 2-cycloocten-1-ol, 2-cycloocten-1-one, and trace amounts of 1,2-cyclooctanediol.

Catalyst activity test

General procedure

EB oxidation reactions were conducted in the dark in a three-necked cylindrical reactor equipped with a fine frit glass disperser tube (Chemglass Life Sciences) and a condenser maintained at −10°C. In a typical reaction, 7 ml of EB, 1 ml of decane, and 3 ml of filtrate (Au + cC_8=OOH-*x* or cC_8=OOH-*x*) were loaded into the reactor together with a Teflon-coated magnetic stirrer. If used, 32 mg of 5% Co/ZSM-5, unless specified otherwise, was added. After the reaction setup was assembled, the reaction mixture was stabilized under N_2 flow for 20 min in a preheated oil bath. Once the temperature of the condenser and oil bath was stabilized, a constant O_2 flow was supplied at 30 ml/min. The reaction mixture (0.1 ml) was taken at different time intervals for analysis (syringe filter was used when solid catalysts were involved), dissolved in 0.7 ml of D-chloroform, and analyzed by ^{1}H nuclear magnetic resonance (NMR).

Product identification and quantification

Aliquots of the reaction mixture were diluted with tetrahydrofuran and analyzed by gas chromatography–mass spectrometry (GC-MS; Agilent GC-7890A, MS-5975). For EB reaction, acetophenone and 1-phenylethanol were identified to be the dominant products. ^{1}H-NMR and ^{13}C-NMR (400 MHz Agilent DD2-MR400 system) were used to further confirm the product identities. 1-Phenylethyl hydroperoxide, which was not detected by GC-MS because of its thermal instability, was identified by NMR to be another dominant product. All three products were quantified by ^{1}H-NMR using decane as the internal standard (fig. S1). The evaporative loss was determined separately and used to correct the product concentrations. After correcting for the evaporative losses, no carbon imbalance was observed for EB reaction. For cyclooctene reaction, cyclooctene oxide, cyclooctane-1,2-diol, 2-cycloocten-1-ol, and 2-cycloocten-1-one were quantified by GC. Cyclooctene 3-hydroperoxide was not stable and decomposed in the GC column and therefore not detected. There was about 10% carbon loss at full conversion even after compensating for the evaporative loss, which could be explained by the formation of small amount of unidentified highly oxidized products.

Conversion and selectivity calculation

GC or NMR area ratio of molecule of interest to the internal standard decane was used to calculate the conversion and selectivity. Although a cooling condenser was used, it was still necessary to compensate for evaporative loss due to high reaction temperature and long reaction time. Evaporative correction curves were obtained for both EB and cC_8= under flowing nitrogen and normalized to the ratio of EB/decane or cC_8=/decane. Because EB and cC_8= have similar boiling points, the normalized correction factors obtained were both 0.0044 (normalized ratio decreased per hour).

Instantaneous evaporative loss from t to $t + T$: $\text{Reactant}_{\text{evp},t\sim t+T} = \text{Reactant}_t * T * 0.0044$.

Accumulative evaporative loss: $\text{Reactant}_{\text{evp}_{\text{sum}},t} = \sum \text{Reactant}_{\text{evp},\,t\sim t+T.}$

Ratio of reactant/decane after correction: $\text{Reactant}_{\text{corr,t}} = \text{Reactant}_t + \text{Reactant}_{\text{evp}_{\text{sum}},t.}$

External conversion: $\text{Conversion}_t = \sum_i \text{Product}_{i,t}/(\sum_i \text{Product}_{i,t} + \text{Reactant}_{\text{corr},t})$.

Product selectivity: $\text{Selectivity}_{i,t} = \text{Product}_{i,t}/\sum_i \text{Product}_{i,t}$.

Carbon loss: $1 - (\sum_i \text{Product}_{i,t} + \text{Reactant}_{\text{corr},t})/\text{Reactant}_{\text{initial}}$.

Quantification of hydroperoxide

The concentration of hydroperoxide was quantified by two titration methods:

1) Triphenylphosphine (PPh_3) titration. PPh_3 (0.1 M in EB) was used to titrate unknown hydroperoxide samples, and the end point was identified with an EM Quant peroxide test strip. ^{31}P-NMR was used to confirm the complete removal of hydroperoxide species.

2) Iodometric titration. Sample (0.2 ml) was mixed together with 1 ml of $CHCl_3$/acetic acid (v/v = 1:2) and 6 ml of 1 M KI solution.

The mixture was stirred in the dark for 2 hours and then titrated with 0.005 M $Na_2S_2O_3$ in the presence of a few drops of starch solution. The end point was reached when the mixture became colorless.

Both methods were internally consistent; however, their results differed by 5 to 10%. Because the Au + cC_8=OOH-*x* and cC_8=OOH-*x* used in this project were generated through cC_8=OOH-initiated oxidation, the hydroperoxide concentration differed from batch to batch but were always within the range 0.2 to 0.5 M for freshly prepared cC_8=OOH-40 to cC_8=OOH-100 samples. The hydroperoxide concentration gradually declined with time of storage.

EPR spin trap experiments

DMPO (23 μl) was added to 1 ml of the sample to reach a DMPO concentration of 0.2 M, and 20 mg of Co/ZSM-5 was added to the sample mixture in a test tube. The mixture was sonicated for 1 min to suspend the catalyst, and this was followed by heating at 60°C for ~10 min. An aliquot of the mixture was transferred into a round borosilicate tubing capillary tube (1.50 inside diameter × 1.80 outside diameter, Wale Apparatus), which had been sealed at one end—this tube was then placed in a Wilmad quartz X-band EPR tube (Sigma-Aldrich). The sample was frozen by immersion of the EPR tube in liquid N_2. Immediately before measuring EPR spectra, the sample was thawed. Continuous-wave (CW) X-band EPR measurements were performed at room temperature on a modified Varian E-4 spectrometer using a finger Dewar.

Isotopic labeling experiment

Deuterated EB (d_{10}-EB) was used in an experiment of a mixture of 6 ml of cC_8=OOH-45, 5 ml of d_{10}-EB, 1 ml of decane, and 60 mg of Co-ZSM-5 (7%), at 120°C, with 6 ml of cC_8=OOH-45, 5 ml of EB-d10, and 1 ml of dodecane. To compensate for the decrease in reaction rate due to the kinetic isotope effect, the co-oxidation was carried out at a higher temperature of 120°C. Aliquots of sample were taken before and after 24 hours of reaction and analyzed by ^{2}H-NMR and GC-MS.

The ^{2}H-NMR spectrum (fig. S5, spectrum 2) showed several new peaks after reaction, not present before reaction, at δ1.50, δ1.58, δ4.94, δ7.42 to δ7.72, and δ8.04. Because of the reduced J-coupling constant and sensitivity of ^{2}H-NMR, the splitting patterns were not resolved. The peaks at δ8.04 and δ7.42 to δ7.72 were assigned to the deuterons of the aromatic ring of acetophenone; the peaks at δ1.50 and δ4.94 were assigned to the methyl and benzylic deuteron of 1-phenylethanol, respectively; and the peak at δ1.58 was assigned to the deuteron in D_2O formed from hydroperoxide decomposition. No deuteron was found associated with products of cyclooctene epoxidation, and the formation of deuterated water indicated that the dominant radical chain carriers in the co-oxidation reaction were peroxy and alkoxy based.

GC-MS spectra of the products are shown in fig. S6. Acetophenone-d_8 (m/e 128, fully deuterated, fig. S6A, m/e 127 and 126) were observed. From the cracking pattern, all H-D exchange took place at the methyl position. In addition, 1-phenylethanol-d_9 (m/e 131) (fig. S6B) was the only deuterated products detected. No deuterium was found in cyclooctene oxide (fig. S6C), the most abundant product from cyclooctene epoxidation. 1-Phenylethanol-d_9 could be formed from reaction of phenylethoxy radical with cyclooctene.

SUPPLEMENTARY MATERIALS

Supplementary material for this article is available at http://advances.sciencemag.org/cgi/content/full/6/5/eaax6637/DC1

Fig. S1. ^{1}H NMR spectra of products of EB oxidation initiated with *c*-C_8OOH-60.
Fig. S2. EB conversions initiated by free radical initiators.
Fig. S3. Effect of Au_n concentration on EB oxidation.
Fig. S4. CW X-band EPR spectra of reaction-generated DMPO radical adducts.
Fig. S5. ^{2}H-NMR before (spectrum 1, red) and after (spectrum 2, green) 24-hour co-oxidation reaction.
Fig. S6. Mass spectra of reaction products in deuterated EB experiments.
Fig. S7. Comparison of initial conversions of 4-methyl anisole initiated using Au + cC8=OOH-100, with cC8=OOH removed.
Fig. S8. Reaction mechanism of simultaneous C8= and EB oxidation after initiation by Au_n.
Table S1. Parameters of various DMPO radical adducts, with previously reported hyperfine couplings.
Table S2. Initial reaction rates.
Table S3. Initial selectivities.
References (*20*, *21*)

REFERENCES AND NOTES

1. R. A. Sheldon, J. K. Kochi, *Metal-Catalyzed Oxidations of Organic Compounds: Mechanistic Principles and Synthetic Methodology Including Biochemical Processes* (Academic Press, 1981).
2. L. Qian, Z. Wang, E. V. Beletskiy, J. Liu, H. J. dos Santos, T. Li, M. d. C. Rangel, M. C. Kung, H. H. Kung, Stable and solubilized active Au atom clusters for selective epoxidation of *cis*-cyclooctene with molecular oxygen. *Nat. Commun.* **8**, 14881 (2017).
3. U. Neuenschwander, I. Hermans, Thermal and catalytic formation of radicals during autoxidation. *J. Catal.* **287**, 1–4 (2012).
4. M. Nowotny, L. N. Pedersen, U. Hanefeld, T. Maschmeyer, Increasing the ketone selectivity of the cobalt-catalyzed radical chain oxidation of cyclohexane. *Chem. Eur. J.* **8**, 3724–3731 (2002).
5. J. Su, C. Xie, C. Chen, Y. Yu, G. Kennedy, G. A. Somorjai, P. Yang, Insights into the mechanism of tandem alkene hydroformylation over a nanostructured catalyst with multiple interfaces. *J. Am. Chem. Soc.* **138**, 11568–11574 (2016).
6. Y. Yamada, C.-K. Tsung, W. Huang, Z. Huo, S. E. Habas, T. Soejima, C. E. Aliaga, G. A. Somorjai, P. Yang, Nanocrystal bilayer for tandem catalysis. *Nat. Chem.* **3**, 372–376 (2011).
7. V. V. Pagar, T. V. RajanBabu, Tandem catalysis for asymmetric coupling of ethylene and enynes to functionalized cyclobutanes. *Science* **361**, 68–72 (2018).
8. R. A. Periana, O. Mironov, D. Taube, G. Bhalla, C. J. Jones, Catalytic, oxidative condensation of CH_4 to CH_3COOH in one step via CH activation. *Science* **301**, 814–818 (2003).
9. B. B. Wentzel, P. L. Alsters, M. C. Feiters, R. J. M. Nolte, Mechanistic studies on the Mukaiyama epoxidation. *J. Org. Chem.* **69**, 3453–3464 (2004).
10. L. Vanoye, J. Wang, M. Pablos, C. de Bellefon, A. Favre-Réguillon, Epoxidation using molecular oxygen in flow: Facts and questions on the mechanism of the Mukaiyama epoxidation. *Cat. Sci. Technol.* **6**, 4724–4732 (2016).
11. *Kirk-Othmer Encyclopedia of Chemical Technology* (John Wiley & Sons Inc., 2018), p. 853.
12. I. Hermans, J. Peeters, P. A. Jacobs, Autoxidation of ethylbenzene: The mechanism elucidated. *J. Org. Chem.* **72**, 3057–3064 (2007).
13. A. A. Gavrichkov, I. V. Zakharov, Critical phenomena in ethylbenzene oxidation in acetic acid solution at high cobalt(II) concentrations. *Russ. Chem. Bull.* **54**, 1878–1882 (2005).
14. G. C. Maikap, D. Guhathakurta, J. Iqbal, Cobalt catalyzed benzylic oxidation with molecular oxygen. *Synlett*, 189–190 (1995).
15. Y. Ishii, T. Iwahama, S. Sakaguchi, K. Nakayama, Y. Nishiyama, Alkane oxidation with molecular oxygen using a new efficient catalytic system: *N*-hydroxyphthalimide (NHPI) combined with $Co(acac)_n$ (n = 2 or 3). *J. Org. Chem.* **61**, 4520–4526 (1996).
16. R. R. O. Brydon, A. Peng, L. Qian, H. H. Kung, L. J. Broadbelt, Microkinetic modeling of homogeneous and gold nanoparticle-catalyzed oxidation of cyclooctene. *Ind. Eng. Chem. Res.* **57**, 4832–4840 (2018).
17. S. I. Dikalov, R. P. Mason, Reassignment of organic peroxyl radical adducts. *Free Radic. Biol. Med.* **27**, 864–872 (1999).
18. M. J. Davies, T. F. Slater, Studies on the photolytic breakdown of hydroperoxides and peroxidized fatty acids by using electron spin resonance spectroscopy. Spin trapping of alkoxyl and peroxyl radicals in organic solvents. *Biochem. J.* **240**, 789–795 (1986).
19. H. Zhu, Z. Ma, J. C. Clark, Z. Pan, S. H. Overbury, S. Dai, Low-temperature CO oxidation on Au/fumed SiO_2-based catalysts prepared from $Au(en)_2Cl_3$ precursor. *Appl. Catal. A Gen.* **326**, 89–99 (2007).
20. E. G. Janzen, G. A. Coulter, U. M. Oehler, J. P. Bergsma, Solvent effects on the nitrogen and β-hydrogen hyperfine splitting constants of aminoxyl radicals obtained in spin trapping experiments. *Can. J. Chem.* **60**, 2725–2733 (1982).
21. E. G. Janzen, J. I.-P. Liu, Radical addition reactions of 5,5-dimethyl-1-pyrroline 1-oxide. ESR spin trapping with a cyclic nitrone. *J. Magnetic Resonance* **9**, 510–512 (1973).

Acknowledgments: We thank B. Hoffman for helpful discussions. **Funding:** This study was supported by the U.S. Department of Energy, Office of Science, Office of Basic Energy Sciences under award number DOE DE-FG02-03-ER15457. EPR experiments were supported by the NIH (grant NH13531). **Author contributions:** A.P. collected most of the data and contributed significantly to the design of experiments and interpretation of data and preparation of the manuscript. L.Q. made the initial observations that formed the basis of the investigation. M.C.K. and H.H.K. contributed significantly to the design of experiments and interpretation of data and preparation of the manuscript. R.R.O.B. and L.J.B. were responsible for providing the detailed reaction mechanism. M.O.R. was responsible for the EPR experiments and their interpretation. **Competing interests:** The authors declare that they have no competing interest. **Data and materials availability:** All data needed to evaluate the conclusions in the paper are present in the paper and/or the Supplementary Materials. Additional data related to this paper may be requested from the authors.

Submitted 11 April 2019
Accepted 21 November 2019
Published 31 January 2020
10.1126/sciadv.aax6637

Citation: A. Peng, M. C. Kung, R. R. O. Brydon, M. O. Ross, L. Qian, L. J. Broadbelt, H. H. Kung, Noncontact catalysis: Initiation of selective ethylbenzene oxidation by Au cluster-facilitated cyclooctene epoxidation. *Sci. Adv.* **6**, eaax6637 (2020).